RESEARCH ARTICLE

miRNA-449a is downregulated in osteosarcoma and promotes cell apoptosis by targeting BCL2

Jie Chen[1] · Jinsong Zhou[1,2] · Xin Chen[1] · Baohui Yang[1] · Dong Wang[1] · Pinglin Yang[1] · Xijing He[1] · Haopeng Li[1]

Abstract Accumulating evidence reveals that miR-449a is expressed at a low level in several tumors and cancer cell lines, and acts as a tumor suppressor in several cancers. However, its role in osteosarcoma (OS) is not well understood. In the present study, we found that miR-449a was significantly downregulated in both OS tissues and cell lines. Furthermore, low expression level of miR-449a was correlated with advanced tumor stage, metastasis, and predicted a poor overall survival in OS patients. Additionally, restoration of miR-449a in OS cell lines U2OS and Saos-2 reduced cell viability, promoted cell apoptosis in vitro, and suppressed tumorigenicity in vivo. Moreover, BCL2, an antiapoptotic molecule, was identified to be a direct target of miR-449a, and the proapoptotic function of miR-449a was mainly through targeting BCL2 expression. Taken together, our results demonstrated a tumor-suppressive role of miR-449a in OS progression and suggested a potential therapeutic target for OS.

Keywords miR-449a · Osteosarcoma · Tumor suppressor · Apoptosis · BCL2

Jie Chen and Jinsong Zhou contributed equally to this work.

✉ Haopeng Li
hpengli305@126.com

1 Department of Orthopaedic Surgery, Second Affiliated Hospital of Medical School of Xi'an Jiaotong University, No. 157 Xiwu Road, Xi'an, Shaanxi 710004, People's Republic of China

2 Department of Orthopaedic Surgery, Xi'an No. 5 Hospital, Xi'an, Shaanxi 710004, People's Republic of China

Introduction

MicroRNAs (miRNAs) are an abundant class of non-coding small RNAs of 17–25 nucleotides that regulate expression of target genes at the post-transcriptional level [1]. MicroRNAs function by directly binding to their potential target site in the 3′ untranslated region (3′UTRs) of the specific target mRNAs, resulting in the repression of mRNA translation or the degradation of target mRNAs [2]. Growing evidence has suggested that miRNAs play key roles in the regulation of diverse biological processes, including cell proliferation, differentiation, as well as cancers [2, 3]. However, dysregulated microRNAs and their roles in cancer carcinogenesis and progression remain largely unknown.

Osteosarcoma (OS) becomes the most common malignant bone tumor with high incidence in children and adolescents [4]. Despite dramatic advances in surgical techniques and chemotherapeutic treatment, the five-year survival rate for patients suffering from OS is only about 50 % [5, 6]. Therefore, it is necessary to improve current therapeutic modalities and to explore new biological molecular markers for predicting the progression of OS and helping targeted therapy. Recent researches have provided evidences that dysregulated miRNAs are greatly involved in the pathogenesis of OS. Both upregulation and downregulation of specific miRNAs have been described in OS carcinogenesis and progression, such as upregulated miR-135b [7], miR-214 [8], and miR-17–92 [9] and downregulated miR-142 [10], miR-144 [11], and miR-145 [12]. However, the precise role of miRNAs in OS development and progression remains unclear.

Recently, miR-449a has been reported to be downregulated in several cancer cell lines and solid tumors including prostate cancer [13], gastric cancers [14, 15], colorectal cancer [16], and lung cancer [17, 18]. miR-449a could inhibit cell growth and induce cell apoptosis and senescence by regulation of key

factors in cell cycle and apoptosis such as histone deacetylase 1 (HDAC1) [13], cyclin D1 (CCND1) [14], CDC25A [19], and CDK6 [15]. However, whether miR-449a is dysregulated in osteosarcoma and its roles in osteosarcoma carcinogenesis and progression are still elusive.

In the current study, we found that miR-449a was downregulated in OS tissues and cell lines, and low expression level of miR-449a was associated with advanced tumor stage and metastasis and predicted a poor overall survival in OS. Restoration of miR-449a expression in OS cell lines reduced cell viability and promoted cell apoptosis in vitro and suppressed tumorigenicity in vivo. In addition, BCL2 was confirmed as a direct target of miR-449a, and the proapoptotic function of miR-449a may be through targeting BCL2 expression. Thus, our data suggest that miR-449a might be a promising therapeutic target for OS.

Material and methods

Patients and tumor specimens

Fresh surgically resected osteosarcoma tumor tissues and corresponding normal adjacent tissue (NAT) were obtained from 60 patients at the Department of Orthopaedic Surgery, Second Affiliated Hospital of Medical School of Xi'an Jiaotong University, between January 2010 and November 2011. None of the patients received preoperative chemotherapy or radiotherapy before surgery. Clinicopathological characteristics of OS patients were detailed in Table 1. Surgically removed tissues were quickly frozen in liquid nitrogen until use. This study was approved by the Research Ethics Committee of Medical School of Xi'an Jiaotong University, People's Republic of China. Written informed consent was obtained from all of the patients according to committee's regulations.

Animals and cell lines

Female BALB/c nu/nu mice (6–8 weeks old) were purchased from Shanghai Laboratory Animal Center (Shanghai, China) and housed in specific pathogen-free conditions. All animals received humane care according to the criteria outlined in the "*Guide for the Care and Use of Laboratory Animals*" prepared by the National Academy of Sciences and published by the National Institutes of Health (NIH publication 86–23 revised 1985). Human osteosarcoma cell lines (MG-63, U2OS, HOS, and Saos-2), human normal osteoblastic cell line hFOB 1.19, and normal human osteoblast cells NHOst were purchased from American Type Culture Collection (ATCC; Rockville, MD, USA). Cells were cultured in Dulbecco's Modified Eagle's Medium (Gibco BRL, Grand Island, NY) containing 10 % fetal bovine serum, penicillin (100 U/mL),

Table 1 Association between miR-449a expression and clinicopathological features of 60 OS patients

Characteristics	Cases (60)	miR-449a expression		P value
		Low (34)	High (26)	
Age (years)				
≤18	32	21	11	
>18	28	13	15	0.216
Gender				
Male	31	15	16	
Female	29	19	10	0.281
Tumor site				
Femur/tibia	43	23	20	
Others	17	11	6	0.616
Tumor stage				
I+II	30	10	20	
III	30	24	6	0.001
Tumor diameter (cm)				
≤6	39	25	14	
>6	21	9	12	0.190
Distant metastasis				
Yes	24	19	5	
No	36	15	21	0.009
Differentiation status				
High	34	20	14	
Low	26	14	12	0.902

and streptomycin (100 μg/mL) at 37 °C in a humidified incubator containing 5 % CO_2.

RNA extraction and real-time quantitative RT-PCR

Total RNA, including miRNA, were extracted from tumor tissues and cells using miRNeasy Kit (QIAGEN, Valencia, CA, USA) according to manufacturer's instructions. Mature miRNAs were converted into cDNA using PrimeScript RT Reagent Kit with gDNA Eraser (TaKaRa, Japan) and miRNA-specific stem-loop RT primer (Applied Biosystems, USA). For the synthesis of cDNA, the reaction mixture was incubated at 42 °C for 15 min, 85 °C for 5 s, and then held at 4 °C. Quantitative reverse transcriptase polymerase chain reaction (qRT-PCR) was performed on ABI 7500 Fast Real-Time PCR System (Applied Biosystems, USA) using SYBR Premix Ex Taq TM II (TaKaRa, Japan) according to manufacturer's instructions. Stem-loop RT primer for miR-143 was 5′-GTCGTATCCAGTGCAGGGTCCGAGGTATTCGCACTG GATACGATACCAGCT-3′, and qRT-PCR primers for miR-449a were 5′-TGGCGGTGGCAGTGTATTGTTA-3′ (forward) and 5′-GTGCAGGGTCCGAGGT-3′ (reverse). qRT-PCR primers for internal control U6 small nuclear RNA were 5′-GCTTCGGCAGCACATATACTAAAAT-3′

(forward) and 5′-CGCTTCACGAATTTGCGTGTCAT-3′ (reverse); the reverse primer of U6 was used for RT reaction. The relative expression level of miR-449a was normalized to that of internal control U6 by using $2^{-\Delta\Delta Ct}$ cycle threshold method. Each sample was analyzed in triplicate, and the mean expression level was calculated.

Cell transfection

The day before transfection, 2×10^5 cells were seeded into 6-well plate in growth medium without antibiotics at a density of 30–40 % and incubated overnight. The transfection of hsa-miR-449a mimic (sense: 5′-UGCGAGUG UAUUGUAAGGUGCU-3′, antisense: 5′-CACGUAAC AUUA CACGUCCAUU-3′) and mimic negative control RNA (5′-ACAUCUGAUGCA CAGUGGAdTdT-3′, antisense 5′-UGUACUCUCAUUCAGCAGUdTdT-3) chemically synthesized by RiboBio (Guangzhou, China) was performed using HiPerFect Transfection Reagent (QIAGEN, Hilden, German) according to manufacturer's protocol. The mixture was added to cells at a final concentration of 100 nM. In addition, BCL2 stably overexpressed U2OS and Saos-2 were transfected and selected in 600 μg/mL G418 for 4 weeks and then confirmed by Western blot for BCL2 expression.

Cell viability assay

Cells were seeded into 96-well plates at 5×10^3 cells per well and cultured for indicated time points. Cell viability was evaluated using CCK-8 (Beyotime, Haimen, China) according to manufacturer's instructions. OD values were read using a microplate reader (BioTek Company, Winooski, VT, USA) at the 450-nm wavelength. Each time point was repeated in three wells, and the experiment was independently performed for three times.

Cell apoptosis assay

Cell apoptosis was evaluated by flow cytometry using an Annexin V-FITC Apoptosis Detection Kit (KeyGen Biotech Co. Roche, Nanjing, China). Briefly, the group and cell culture were the same as above. Forty eight hours after transfection, cell culture medium was replaced by fresh serum-free DMEM and cells were cultured for an additional 48 h; then the cells were detached by trypsinization, washed twice in PBS, and resuspended in 500 μL binding buffer. A volume of 5 μL Annexin V-FITC and 5 μL propidium iodide was added and mixed gently, and the cells were stained in the dark for 10 min at room temperature. The cells were analyzed immediately by flow cytometry (BD FACS Calibur, BD Bioscience, San Diego, CA) and analyzed using FlowJo software (FlowJo, Ashland, OR). The experiment was repeated three times.

In vivo tumorigenicity assay

For evaluation of the tumor growth in vivo, mimic control or miR-449a mimic-transfected U2OS and Saos-2 cells (2×10^6) were suspended in 0.1 mL PBS and then injected subcutaneously into the flank region of 6–8-week-old female nude mice. Tumor growth was monitored every 5 days, tumors were measured with fine digital calipers, and tumor volume was calculated by the following formula: tumor volume=$0.5\times$width$^2\times$length.

3′UTR luciferase reporter assay

To construct the luciferase reporter plasmid containing BCL2 3′UTR sequence, BCL2 mRNA 3′UTR sequence containing the putative miR-449a binding sequence was amplified by PCR and cloned downstream of the Firefly luciferase gene in the pMIR-Report vector (Promega, Madison, WI, USA) between the HindIII and SpeI sites. Reporter plasmid containing miR-195 target site-deleted BCL2 3′UTR sequence was made by ligation of PCR fragments of BCL2 3′UTR luciferase reporter plasmid lacking the target site. 1×10^4 U2OS and Saos-2 cells were seeded into each well of 96-well plate and co-transfected with 100 ng BCL2 3′UTR Firefly, luciferase reporter plasmid, 20 ng pRL-TK-Renilla-luciferase plasmid, and NC or miR-449a mimic using jetPRIME transfection reagent (Polyplus-transfection). After 48 h, Luciferase activity was measured by using a Dual-Luciferase Reporter Assay (Promega, Madison, WI, USA) on a Fluorescence Spectrophotometer F4500 (Hitachi, Tokyo, Japan). Data were normalized by dividing Firefly luciferase activity with that of Renilla luciferase. All experiments were repeated three times in triplicate.

Western blotting

About 20 μg of total protein was extracted and separated by 10 % SDS-PAGE, transferred onto polyvinylidene fluoride membranes. The primary rabbit monoclonal antibodies to BCL2 (Santa Cruz, CA, USA) and β-actin (Santa Cruz, CA, USA) were incubated with the blot overnight at 4 °C. After being extensively washed with PBS containing 0.1 % Triton X-100, the membranes were incubated with HRP-conjugated goat anti-rabbit antibody for 30 min at room temperature. The bands were visualized using the ECL system (Millipore, Billerica, WI, USA).

Statistical analysis

Statistical analysis was performed with SPSS 16.0 for Windows (SPSS, Chicago, IL).

Data were expressed as means±standard deviation (SD). Paired samples t test was performed to compare the expression levels of miR-449a between osteosarcoma tumor tissues and corresponding normal adjacent tissue. Chi-square test was used to analyze the relationship between miR-449a expression and clinicopathological characteristics. Student's t test was adopted to compare quantitative data. Survival curves were plotted using the Kaplan-Meier product-limit method, and differences between survival curves were tested using the log-rank test. Cox regression analysis in a forward stepwise method was used to evaluate the effect of multiple independent prognostic factors on survival outcome. Differences were considered to be statistical significant when P value was less than 0.05.

Results

miR-449a was downregulated in human OS tissues and correlated with tumor stage and metastasis

We first analyzed miR-449a expression in 60 OS specimens and corresponding normal adjacent tissues (NATs) by qRT-PCR. As shown in Fig. 1, the expression level of miR-449a was significantly downregulated in OS tissues compared with that in NATs ($P < 0.0001$, Fig. 1a).
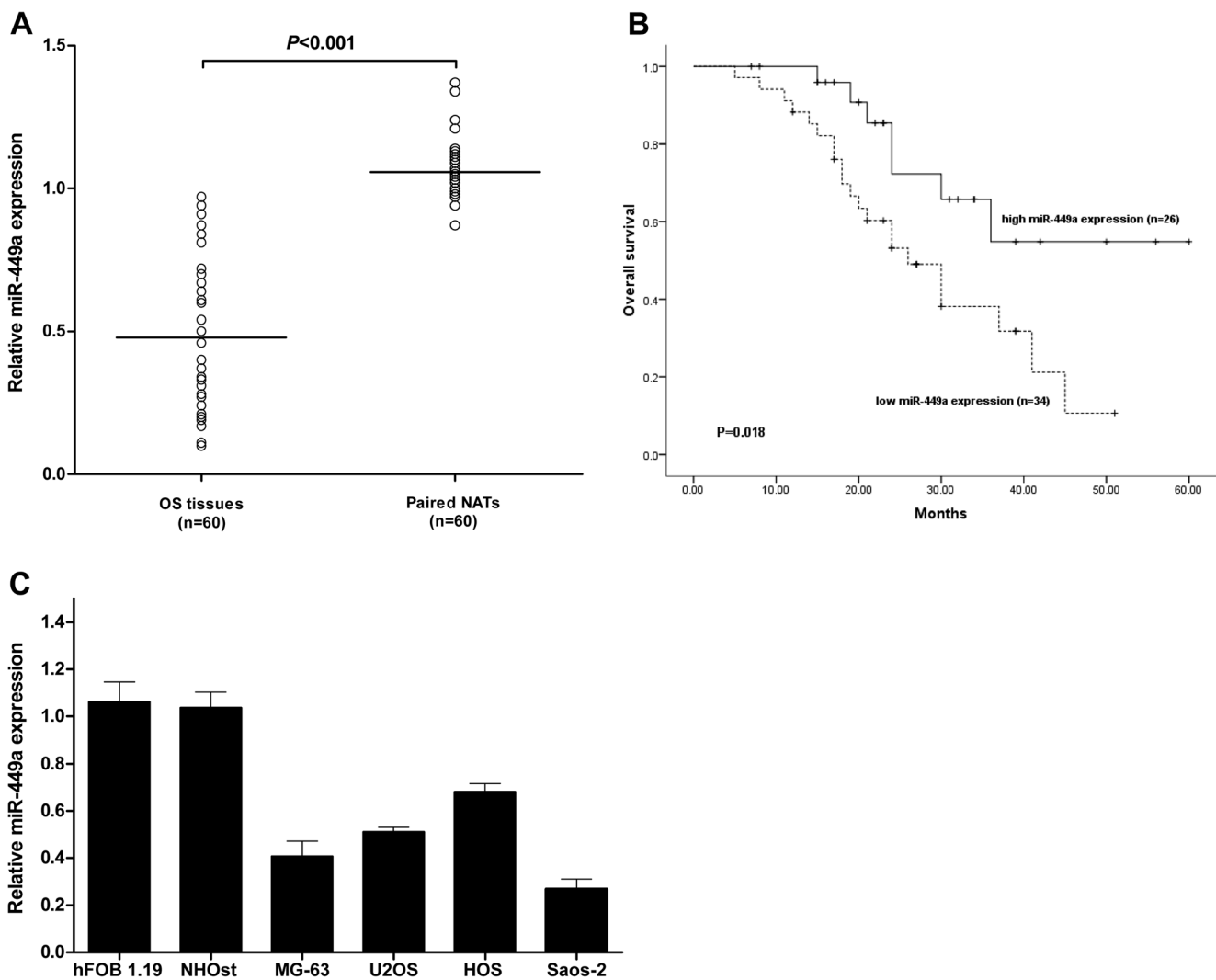

Fig. 1 miR-449a was downregulated in human OS tissues and cell lines. **a** miR-449a expression in 60 paired OS tumor tissues and corresponding normal adjacent tissue (NATs) was detected by quantitative real-time polymerase chain reaction (*qRT-PCR*). **b** Kaplan-Meier curve for OS patients classified as high or low miR-449a expression. The P value was calculated using the log-rank test. **c** miR-449a expression in human OS cell lines (MG-63, U2OS, HOS, and Saos-2), and normal osteoblastic cell lines hFOB 1.19 and NHOst were detected by qRT-PCR

To determine the effects of miR-449a expression on tumor progression, comparisons of the clinical pathological variables with miR-449a expression in OS tissues were made. OS tissues expressing miR-449a at levels less than the mean expression level ($2^{-\Delta\Delta Ct}=0.478$) were assigned to the low expression group (mean expression value 0.290, $n=34$), and those samples with expression above the mean value were assigned to the high expression group (mean expression value 0.723, $n=26$). As shown in Table 2, low levels of miR-449a expression were associated with advanced tumor stage and distant metastasis ($P=0.001$ and $P=0.009$, respectively). However, there was no statistically significant correlation between miR-449a expression and age ($P=0.216$), gender ($P=0.281$), tumor site ($P=0.616$), tumor diameter ($P=0.190$), and differentiation status ($P=0.902$).

Correlation between miR-449a expression and prognosis of OS patients

As shown in Fig. 1b, Overall survival of patients with low miR-449a expression was significantly shorter than survival of those with high miR-449a expression ($P=0.018$). Univariate analysis showed that tumor stage, distant metastasis, and miR-449a expression were predictive factors for poor prognosis of patients with OS ($P<0.001$, $P=0.004$, and $P=0.001$, respectively; Table 2). Multivariate analysis showed that expression level of miR-449a ($P=0.017$, hazard ratio (HR)= 0.824, 95 % confidence interval (CI) 0.374–1.277) was an independent prognostic factor independent of other clinicopathologic factors, for instance, tumor stage and distant metastasis (Table 2).

miR-449a was downregulated in OS cell lines and affected cell proliferation, apoptosis, and tumorigenicity

We then examined the expression of miR-449a in four human OS cell lines MG-63, U2OS, HOS, and Saos-2 and two normal osteoblastic cell lines hFOB 1.19 and NHOst by using RT-qPCR. As shown in Fig. 1c, compared to the normal osteoblastic cells, all four OS cell lines showed significant downregulation of miR-449a.

We then explored the potential effects of miR-449a on cell growth in vitro and in vivo. To determine the effect of miR-449a on cell proliferation and apoptosis, U2OS and Saos-2 cells were transfected with mimic control and miR-449a mimic. As shown in Fig. 2a, b, restoration of miR-449a decreased cell viability in both of the OS cell lines. In addition, restoration of miR-449a promoted cell apoptosis in U2OS and Saos-2 cells (Fig. 2c, d). We next investigated the effect of miR-449a restoration on tumorigenicity in vivo. As shown in Fig. 2e, f, miR-449a overexpression remarkably suppressed tumor growth compared to that of mimic controls. However, we did not found a cytotoxic effect of miR-449a overexpression on normal osteoblast cells (Fig. S1 A–D).

BCL2 was a direct target of miR-449

In order to further investigate the mechanisms responsible for the apoptosis-promoting effect of miR-449a on OS, we next sought to identify the molecular targets of miR-449a. TargetScan 6.2 was used to screen the potential target gene of miR-449a. Of the hundreds of predicted target genes in TargetScan, we found that human BCL2, an important antiapoptotic molecule, contained conserved putative miR-449a target site (Fig. 3a). To determine whether BCL2 is directly targeted by miR-449a expression, we constructed luciferase reporter plasmids containing BCL2 3′UTR or bearing deletion of the putative miR-449a target site. By co-transfection with miR-449a mimic, we found that the luciferase activity of the full-length BCL2 3′UTR reporter was suppressed, while target site-deleted reporter failed to be targeted by miR-449a co-transfection (Fig. 3b). In addition, endogenous protein expression of BCL2 was also inhibited by miR-449a expression in U2OS and Saos-2 cells (Fig. 3c). We next compared BCL2 protein expression between human normal osteoblast cell lines and osteosarcoma cell lines. As shown in

Table 2 Univariate and multivariate analyses of overall survival in OS patients

Factors	Univariate			Multivariate		
	Hazard ratio	95 % CI	P	Hazard ratio	95 % CI	P
Age, years (≤18/>18)	0.947	(0.674–1.271)	0.661			
Gender (male/female)	0.994	(0.543–1.520)	0.912			
Tumor diameter (≤6/>6)	1.347	(0.839–2.077)	0.054			
Differentiation status (high/low)	1.173	(0.714–1.804)	0.241			
Tumor stage (I, II/III)	5.574	(2.047–9.115)	<0.001	4.301	(2.121–7.364)	0.002
Distant metastasis (yes/no)	3.017	(1.734–6.721)	0.004	1.942	(1.377–5.540)	0.029
miR-449a expression (low/high)	0.741	(0.423–1.347)	0.001	0.824	(0.374–1.277)	0.017

Fig. 2 miR-449a reduces cell viability, promotes cell apoptosis, and suppresses tumorigenicity. **a, b** U2OS and Saos-2 cells were transfected with mimic control or miR-449a mimic as indicated. Cell viability was measured in the indicated time points post transfection using CCK-8 assay. **c, d** Cell apoptosis was detected 48 h post serum deprivation using Annexin V-FITC Apoptosis Detection Kit. **e, f** Mimic control or miR-449a mimic-transfected U2OS and Saos-2 cells were injected subcutaneously into the flank region of 6–8-week-old female nude mice. Tumor growth was monitored every 5 days, and tumor growth curve was shown as indicated. Data shown are mean± SD from three independent experiments. *$P<0.05$, **$P<0.01$, ***$P<0.001$
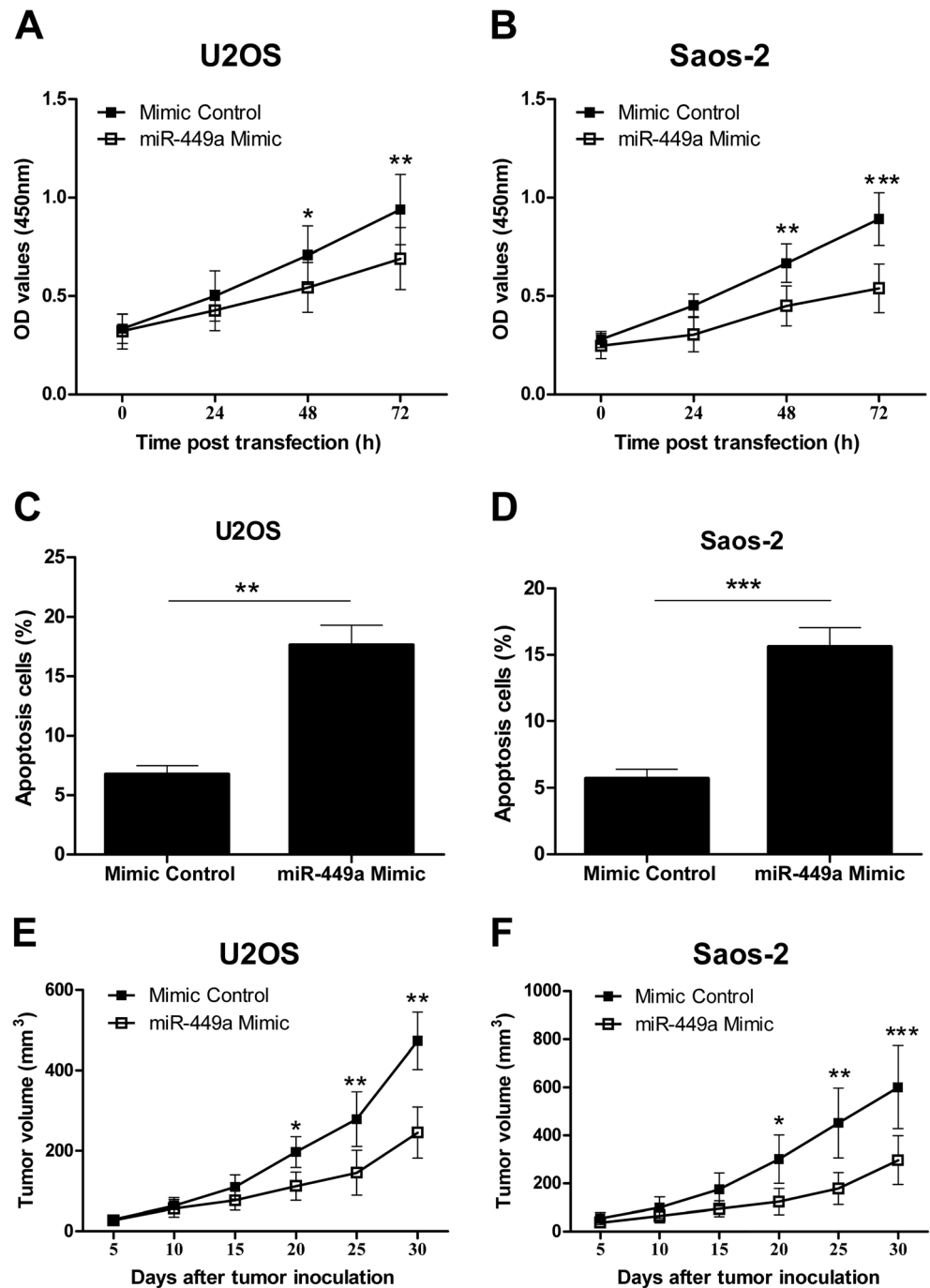

Fig. S1E, BCL2 protein expression was significantly down-regulated in normal osteoblast cell lines in comparison to that in osteosarcoma cell lines. We further compared BCL2 expression in paired human OS tissues and found that BCL2 protein level was also upregulated in miR-449a downregulated OS tissues (Fig. 3d). Taken together, these data demonstrate that BCL2 is a direct target of miR-449a and further suggest that miR-449a may exert its apoptosis-promoting effect through inhibition of BCL2 expression.

To further confirm the proapoptotic effect of miR-449a which was through targeting BCL2, we constructed BCL2 stably overexpressed OS U2OS and Saos-2 cells without 3′UTR sequence; thus, miR-449a could no longer target BCL2 expression. BCL2 overexpression was confirmed to be elevated by Western blot (Fig. 4a). We found that cell apoptosis promoted by miR-449a was significantly suppressed in BCL2 stably transfected OS cells (Fig. 4b).

Fig. 3 BCL2 was a direct target of miR-449. **a** Sequence alignment of miR-449a and its conserved target site in 3′UTR of BCL2. **b** U2OS and Saos-2 cells were co-transfected with human BCL2 3′UTR Firefly luciferase reporter plasmid or miR-449a target site-deleted reporter plasmid, together with mimic control or miR-449a mimic plasmids as indicated. After 48 h, Firefly luciferase activity was measured and normalized by Renilla luciferase activity. **c** U2OS and Saos-2 cells were transfected as described in Fig. 2a. After 48 h, human BCL2 was detected by Western blot. **d** Expression of BCL2 in paired human OS tissues was detected by Western blot. miR-449a expression in these samples was also shown. Data shown are mean ±SD from three independent experiments. **P<0.01
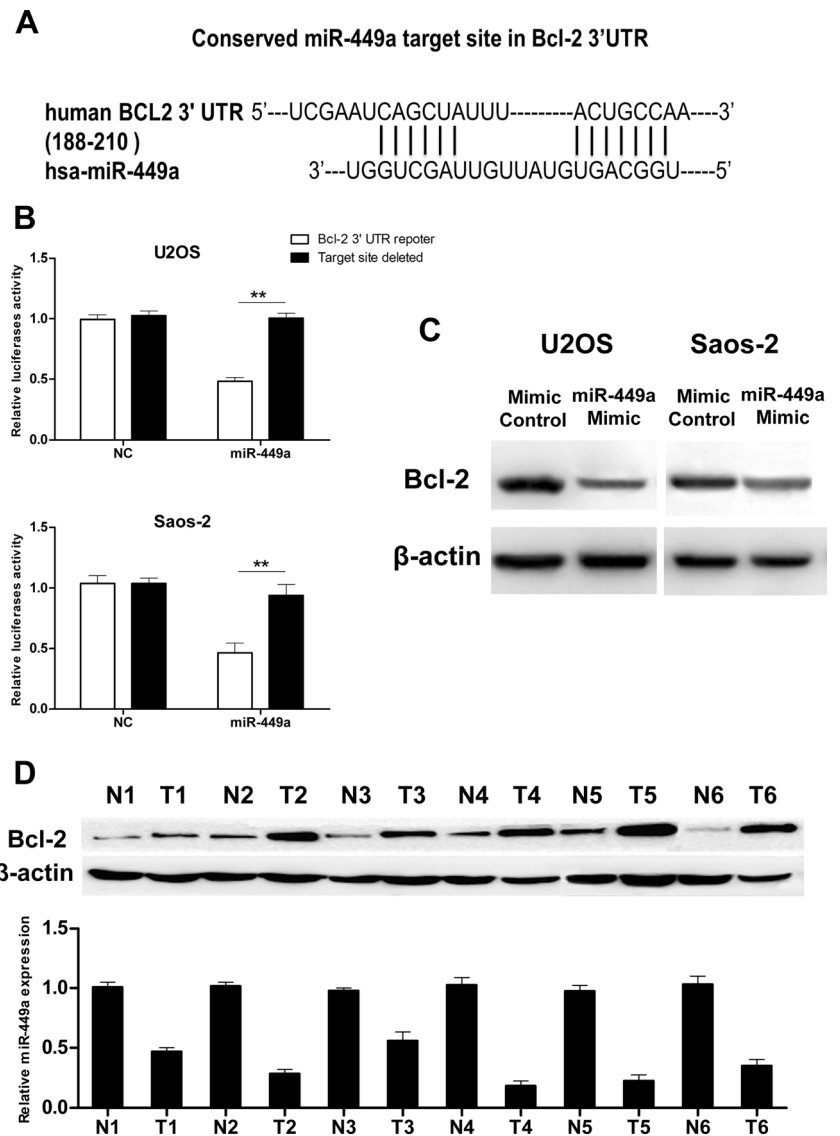
Discussion

It is supposed that downregulated miRNAs in cancers may function as tumor-suppressor genes and vice versa [20]. Given that miR-449a has been reported to be underexpressed in

several malignant tumors and cancer cell lines, we presumed that miR-449a may be a tumor inhibitor in osteosarcoma. In the present study, we found that miR-449a was significantly decreased in OS tissues and cell lines, which was consistent with the precious reports in other malignant tumors. In
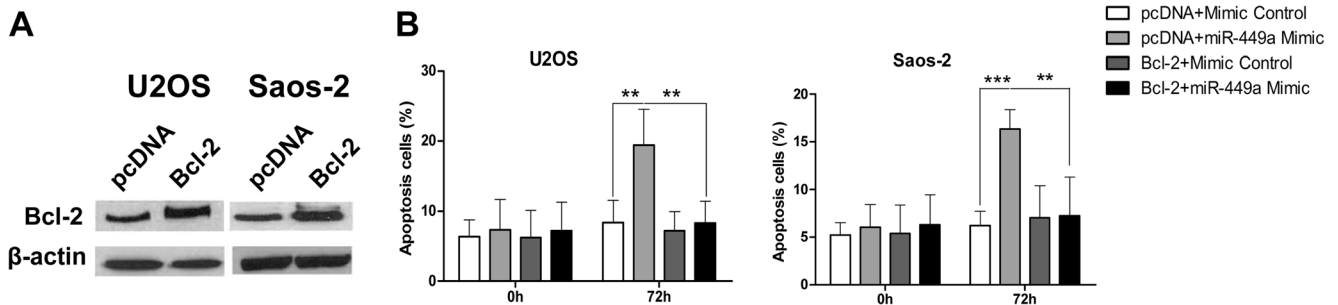
Fig. 4 Proapoptotic effect of miR-195 is mainly through targeting BCL2. **a** BCL2 expression in empty pcDNA vector or BCL2 expressing plasmid stably transfected U2OS and Saos-2 cells was detected by Western blot. **b** U2OS and Saos-2 in **a** were transfected as described in Fig. 2a. Cell apoptosis was measured 72 h post serum deprivation. Data shown are mean±SD from three independent experiments. **P<0.01, ***P<0.001

addition, we found that low levels of miR-449a expression were associated with advanced tumor stage and distant metastasis. To our knowledge, our results indicated for the first time that miR-449a was associated with tumor stage and metastasis in OS. Moreover, follow-up data showed that five-year overall survival of patients with low miR-449a expression was significantly shorter than survival of those with high miR-449a expression, and low expression level of miR-449a was an independent prognostic factor. These results indicated that miR-449a may be a novel useful prognosis predictor independent of other clinicopathologic factors for patients with OS. In combination with previous reports revealing the roles of miR-449a in some other types of cancer, we further confirmed that miR-449a may function as a tumor suppressor.

The tumor-suppressive roles of miR-449a in OS were further confirmed both in vitro and in vivo. In the CCK-8 and apoptosis assays, it was shown that restoration of miR-449a inhibited cell proliferation and promoted cell apoptosis in OS U2OS and Saos-2 cells. We next investigated the effect of miR-449a restoration on tumorigenicity in vivo. We found that miR-449a overexpression remarkably suppressed tumor growth compared to that of mimic controls. Taken together, our data suggest that miR-449a inhibits tumorigenicity of OS cells in vitro and in vivo and further suggest the tumor-suppressive role of miR-449a in OS. Our results were also consistent with those in previous studies in gastric adenocarcinoma and bladder cancer [21, 22].

miR-449a could inhibit cell growth and induce cell apoptosis and senescence by regulation of key factors in cell cycle and apoptosis. However, the precise molecular mechanisms for the downregulation of miR-449a in OS remain unknown. Of the hundreds of potential target genes for miR-449a predicted by TargetScan, the antiapoptotic BCL2 was selected for study. Most recently, BCL2 has already been identified as target of miR-449a by luciferase reporter assay in MGC-803 and SGC-7901 gastric adenocarcinoma cell lines [21]. Our results agree with the observation that BCL2 is a direct target of miR-449a. We demonstrated an inverse correlation between miR-449a and BCL2 in OS tissues. In vitro overexpression of miR-449a in OS cell lines significantly decreased BCL2 expression. Furthermore, luciferase reporter assay demonstrated that miR-449a directly bound to the BCL2 3′UTR region, suggesting that miR-449a may exert its proapoptotic function via inhibiting BCL2 expression.

BCL2, an important antiapoptosis regulator protein, inhibits cell apoptosis through the mitochondrial pathway and plays a crucial role in cell viability [23]. Loss of BCL2 gene has been identified as a cause of a number of cancers, including OS, and correlates with prognostic parameters and poor survival in OS [24, 25]. BCL2 is also well accepted to protect osteosarcoma cells from apoptosis [26, 27]. In the present study, we further investigated whether the proapoptotic function of miR-449a was mainly through targeting BCL2. We

prepared BCL2 stably overexpressed U2OS and Saos-2 cells which expressed BCL2 mRNA without its 3′UTR sequence. We found that cell apoptosis promoted by miR-449a was significantly suppressed in BCL2 stably transfected OS cells. Accordingly, by directly targeting the gene BCL2, miR-449a inhibited BCL2 expression and downstream caspases 3 and 7 activation, then induced cell apoptosis. Our data provide the first insights into the function of miR-449a in regulating cell apoptosis in OS cells, at least partially through BCL2. However, as there were hundreds of predicted targets of miR-449a discovered in the TargetScan prediction, and a single miRNA has been proven to target multiple mRNAs to post-transcriptional regulation, it is probable that other targets of miR-449a may also participate in OS carcinogenesis. Therefore, further studies are needed to identify the entire role of miR-449a in OS progression.

In conclusion, the present results showed that miR-449a, a significantly downregulated miRNA in OS, was associated with advanced tumor stage and poor prognosis. We also demonstrated that miR-449a played a crucial role in inducing apoptosis by directly targeting BCL2. Although the precise molecular mechanisms require further study, miR-449a provides new insights into prognostic diagnosis and therapeutic strategies for patients with OS.

Conflicts of interest None

References

1. Lee RC, Feinbaum RL, Ambros V. The C. elegans heterochronic gene lin-4 encodes small RNAs with antisense complementarity to lin-14. Cell. 1993;75(5):843–54.
2. Bartel DP. MicroRNAs: genomics, biogenesis, mechanism, and function. Cell. 2004;116(2):281–97.
3. Lu J, Getz G, Miska EA, Alvarez-Saavedra E, Lamb J, Peck D, et al. MicroRNA expression profiles classify human cancers. Nature. 2005;435(7043):834–8. doi:10.1038/nature03702.
4. Gill J, Ahluwalia MK, Geller D, Gorlick R. New targets and approaches in osteosarcoma. Pharmacol Ther. 2013;137(1):89–99. doi:10.1016/j.pharmthera.2012.09.003.
5. Botter SM, Neri D, Fuchs B. Recent advances in osteosarcoma. Curr Opin Pharmacol. 2014;16:15–23. doi:10.1016/j.coph.2014.02.002.
6. Wu PK, Chen WM, Lee OK, Chen CF, Huang CK, Chen TH. The prognosis for patients with osteosarcoma who have received prior manipulative therapy. J Bone Joint Surg (Br). 2010;92(11):1580–5. doi:10.1302/0301-620X.92B11.24706.
7. Pei H, Jin Z, Chen S, Sun X, Yu J, Guo W. MiR-135b promotes proliferation and invasion of osteosarcoma cells via targeting FOXO1. Mol Cell Biochem. 2015;400(1–2):245–52. doi:10.1007/s11010-014-2281-2.
8. Xu Z, Wang T. miR-214 promotes the proliferation and invasion of osteosarcoma cells through direct suppression of LZTS1. Biochem

Biophys Res Commun. 2014;449(2):190–5. doi:10.1016/j.bbrc.2014.04.140.

9. Arabi L, Gsponer JR, Smida J, Nathrath M, Perrina V, Jundt G, et al. Upregulation of the miR-17-92 cluster and its two paraloga in osteosarcoma—reasons and consequences. Genes Cancer. 2014;5(1–2):56–63.

10. Zheng Z, Ding M, Ni J, Song D, Huang J, Wang J. miR-142 acts as a tumor suppressor in osteosarcoma cell lines by targeting Rac1. Oncol Rep. 2014. doi:10.3892/or.2014.3687.

11. Zhao M, Huang J, Gui K, Xiong M, Cai G, Xu J, et al. The down-regulation of miR-144 is associated with the growth and invasion of osteosarcoma cells through the regulation of TAGLN expression. Int J Mol Med. 2014;34(6):1565–72. doi:10.3892/ijmm.2014.1963.

12. Li E, Zhang J, Yuan T, Ma B. MiR-145 inhibits osteosarcoma cells proliferation and invasion by targeting ROCK1. Tumour Biol. 2014;35(8):7645–50. doi:10.1007/s13277-014-2031-9.

13. Noonan EJ, Place RF, Pookot D, Basak S, Whitson JM, Hirata H, et al. miR-449a targets HDAC-1 and induces growth arrest in prostate cancer. Oncogene. 2009;28(14):1714–24. doi:10.1038/onc.2009.19.

14. Hu J, Fang Y, Cao Y, Qin R, Chen Q. miR-449a Regulates proliferation and chemosensitivity to cisplatin by targeting cyclin D1 and BCL2 in SGC7901 cells. Dig Dis Sci. 2014;59(2):336–45. doi:10.1007/s10620-013-2923-3.

15. Li LP, Wu WJ, Sun DY, Xie ZY, Ma YC, Zhao YG. miR-449a and CDK6 in gastric carcinoma. Oncol Lett. 2014;8(4):1533–8. doi:10.3892/ol.2014.2370.

16. Chen S, Dai Y, Zhang X, Jin D, Li X, Zhang Y. Increased miR-449a expression in colorectal carcinoma tissues is inversely correlated with serum carcinoembryonic antigen. Oncol Lett. 2014;7(2):568–72. doi:10.3892/ol.2013.1737.

17. Ding M, Qiu TF, Zhou PG. microRNA-449a suppresses non-small cell lung cancer. Cell Biochem Biophys. 2014. doi:10.1007/s12013-014-0339-0.

18. Luo W, Huang B, Li Z, Li H, Sun L, Zhang Q, et al. MicroRNA-449a is downregulated in non-small cell lung cancer and inhibits migration and invasion by targeting c-Met. PLoS ONE. 2013;8(5), e64759. doi:10.1371/journal.pone.0064759.

19. Ye W, Xue J, Zhang Q, Li F, Zhang W, Chen H, et al. MiR-449a functions as a tumor suppressor in endometrial cancer by targeting CDC25A. Oncol Rep. 2014;32(3):1193–9. doi:10.3892/or.2014.3303.

20. Hayes J, Peruzzi PP, Lawler S. MicroRNAs in cancer: biomarkers, functions and therapy. Trends Mol Med. 2014;20(8):460–9. doi:10.1016/j.molmed.2014.06.005.

21. Wei B, Song Y, Zhang Y, Hu M. microRNA-449a functions as a tumor-suppressor in gastric adenocarcinoma by targeting Bcl2. Oncol Lett. 2013;6(6):1713–8. doi:10.3892/ol.2013.1609.

22. Chen H, Lin YW, Mao YQ, Wu J, Liu YF, Zheng XY, et al. MicroRNA-449a acts as a tumor suppressor in human bladder cancer through the regulation of pocket proteins. Cancer Lett. 2012;320(1):40–7. doi:10.1016/j.canlet.2012.01.027.

23. Weyhenmeyer B, Murphy AC, Prehn JH, Murphy BM. Targeting the anti-apoptotic Bcl2 family members for the treatment of cancer. Exp Oncol. 2012;34(3):192–9.

24. Nedelcu T, Kubista B, Koller A, Sulzbacher I, Mosberger I, Arrich F, et al. Livin and Bcl2 expression in high-grade osteosarcoma. J Cancer Res Clin Oncol. 2008;134(2):237–44. doi:10.1007/s00432-007-0276-z.

25. Kaseta MK, Khaldi L, Gomatos IP, Tzagarakis GP, Alevizos L, Leandros E, et al. Prognostic value of bax, Bcl2, and p53 staining in primary osteosarcoma. J Surg Oncol. 2008;97(3):259–66. doi:10.1002/jso.20913.

26. Lin D, Feng J, Chen W. Bcl2 and caspase-8 related anoikis resistance in human osteosarcoma MG-63 cells. Cell Biol Int. 2008;32(10):1199–206. doi:10.1016/j.cellbi.2008.07.002.

27. Zhao Y, Zhang CL, Zeng BF, Wu XS, Gao TT, Oda Y. Enhanced chemosensitivity of drug-resistant osteosarcoma cells by lentivirus-mediated Bcl2 silencing. Biochem Biophys Res Commun. 2009;390(3):642–7. doi:10.1016/j.bbrc.2009.10.020.